

Exceptional Point of Degeneracy in a Backward-Wave Oscillator with Distributed Power Extraction

Tarek Mealy^{✉,*}, Ahmed F. Abdelshafy^{✉,†} and Filippo Capolino^{✉,‡}

Department of Electrical Engineering and Computer Science, University of California, Irvine, California 92697, USA

 (Received 9 February 2020; accepted 2 June 2020; published 24 July 2020)

We show how an exceptional point of degeneracy (EPD) is formed in a system composed of an electron beam interacting with an electromagnetic mode guided in a slow wave structure (SWS) with distributed power extraction from the interaction zone. Based on this kind of EPD, a regime of operation is devised for backward-wave oscillators (BWOs) as a synchronous and degenerate regime between a backward electromagnetic mode and the charge wave modulating the electron beam. Degenerate synchronization under this EPD condition means that two complex modes of the interactive system do not share just the wave number, but they rather coalesce in both their wave numbers and eigenvectors (polarization states). In principle, this condition guarantees full synchronization between the electromagnetic wave and the beam's charge wave for any amount of output power extracted from the beam, setting the threshold of this EPD-BWO to any arbitrary, desired, value. Indeed, we show that the presence of distributed radiation in the SWS results in having high-threshold electron-beam current to start oscillations, which implies higher power generation. These findings have the potential to lead to highly efficient BWOs with very high output power and excellent spectral purity.

DOI: [10.1103/PhysRevApplied.14.014078](https://doi.org/10.1103/PhysRevApplied.14.014078)

I. INTRODUCTION

Exceptional points of degeneracy (EPDs) are points in parameter space of a system at which two or more eigenmodes coalesce in their eigenvalues (wave numbers) and eigenvectors (polarization states). Since the characterizing feature of an exceptional point is the strong degeneracy of at least two eigenmodes, as implied in Ref. [1], we stress the importance of referring to it as a “degeneracy.” Despite most of the published work on EPDs being related to parity-time (PT) symmetry [2–6], the occurrence of an EPD actually does not require a system to satisfy PT symmetry. Indeed, EPDs have recently been found also in single resonators by just adopting time variation of one of its components [7]. EPDs are also found in uniform waveguides at their cutoff frequencies [8] and in periodic waveguides at the regular band edge (RBE) and at the degenerate band edge (DBE). However, the RBE and DBE are EPDs realized in lossless structures [9–14]. Here, we investigate an EPD that requires both distributed power extraction and gain being simultaneously present in a waveguide, referred to here as the “slow wave structure” (SWS) since its mode is used to interact with an

electron beam. Note that the passivity of the waveguide here is not dominated by dissipative losses, but rather from power that is extracted in a continuous fashion from the SWS. Therefore, modes that propagate in such a waveguide experience exponential decay while they propagate, as if the waveguide was lossy. A particular and well-studied case of simultaneous existence of symmetric gain and loss is based on PT symmetry, which is a special condition that leads to the occurrence of an EPD [2–6], which however requires a spatial symmetry in gain and loss. The EPD considered here is far from that condition, involving two completely different media that support waves, a plasma and a waveguide for electromagnetic waves, but still require their interaction and the simultaneous presence of gain and “loss.” We stress that in this paper the term “loss” is not associated to the damping of energy, but rather refers to a waveguide perspective where energy exits the waveguide in a distributed fashion, a mechanism referred to as distributed power extraction (e.g., distributed radiation) from the interaction zone, for example by realizing a distributed long slot along the SWS or a set of periodically spaced holes as in Fig. 1.

In this paper the linear electron beam is modeled using the description presented in Ref. [15]. Then we use a generalization of the well-established Pierce model [16] to account for the interaction of the electromagnetic (EM) wave in the SWS and the electron beam, assuming small

*tmealy@uci.edu

†abdelsha@uci.edu

‡f.capolino@uci.edu

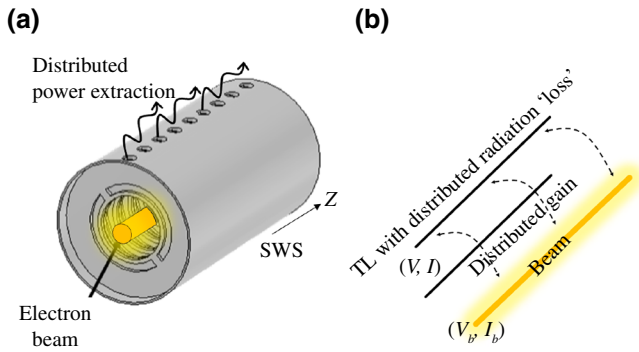


FIG. 1. (a) An example of the SWS with distributed radiating slots that extract power from the guided modes interacting with the electron beam. (b) Pierce-based equivalent transmission line model of the SWS with distributed “loss” (i.e., radiation) coupled to the charge wave modulating the electron beam. From the transmission line point of view, the interaction with the beam is seen as distributed gain.

signal modulation of the beam. The Pierce model consists of an equivalent transmission line (TL) governed by telegrapher’s equations, coupled to a plasmalike medium (the linear electron beam) governed by the equations that describe the electron-beam dynamics. Here we add a distributed load in the Pierce model TL equations that represents the distributed power extraction. Indeed, the distributed radiation coming out of a SWS is conventionally represented by a distributed equivalent “radiation resistance” in a TL, following the well-established terminology used in antenna theory [17–19]. Recently, two coupled transmission lines with balanced gain and loss (balanced refers to the combination that generates an EPD) were shown to support EPDs without the need of PT symmetry [20,21]. Even farther from the usual PT symmetry condition, in this paper the EPD is generated by a TL supporting backward EM wave propagation that interacts with a linear electron beam that is a plasma medium that supports two nonreciprocal waves. We show how this EPD condition can be used in high power electron-beam devices. Backward-wave oscillators (BWOs) are widely used as high power sources in radars, satellite communications, and various other applications. A BWO is composed of a SWS that guides EM backward waves, where their phase and group velocities have opposite directions. The interaction between the electron beam and a backward EM mode constitutes a distributed feedback mechanism that makes the whole system unstable at certain frequencies [22,23]. One of the most challenging issues in BWOs is the limitation in the power generation level, i.e., the extracted power from the electron beam relative to its total power. Indeed, conventional BWOs exhibit a small starting beam current (to induce sustained oscillations) and limited power efficiency, without reaching very high output power levels. The extracted power in a conventional

BWO is taken from one of the SWS waveguide ends. In this paper, we investigate the physics of an EPD resulting from the interaction between an electron beam and an EM mode; moreover, we propose to use such an EPD to conceive high power sources, and this technique can be used from microwaves to terahertz frequencies. The proposed “degenerate synchronization regime” of operation in a BWO is based on the EPD generated by the simultaneous presence of gain (coming from the electron beam) and continuous distributed power extraction from the EM guided wave (rather than power extraction from the waveguide end). Therefore, we stress that the term “loss” does not refer to material loss, but rather to a distributed power extraction mechanism (Fig. 1) that in antenna terminology is referred to as “radiation loss,” while the gain is provided by the electron beam interacting with the SWS. The distributed power extraction from the interaction zone occurs either via a distributed set of radiating slots along the SWS (Fig. 1), or alternatively by collecting the distributed extracted power via an adjacent coupled waveguide.

Recently, SWSs exhibiting a DBE, which is an EPD of order four in a *lossless* periodic waveguide, were proposed to enhance the performance of high power devices [24–27]. It is important to point out that the DBE discussed in these previously mentioned works were obtained in the “cold” SWS by exploiting periodicity, and the benefit of such a DBE would gracefully vanish while increasing the electron-beam power. In this paper, instead, we propose an interaction regime where the EPD is maintained in the “hot” SWS, i.e., in the presence of the interacting electron beam, that is a very large source of distributed gain. The degenerate synchronization between the charge wave induced on the electron beam and the EM slow wave occurs at the EPD, making this degenerate synchronization regime a very special condition not explored previously.

II. SYSTEM MODEL

Consider the SWS shown in Fig. 1(a) supporting a Floquet-Bloch mode whose slow wave spatial harmonic interacts with an electron beam, and radiates via a distributed set of slots (radiation occurs via a fast wave spatial harmonic, usually the so-called “–1” harmonic). The configuration in Fig. 1(a) is given as a possible realization, though another one may consist in collecting the power exiting the interaction zone in a distributed fashion by an adjacent waveguide. We assume that the interaction between the SWS mode and the electron beam is modeled via the Pierce small-signal theory of traveling-wave tubes [15,16,28–32] that describes the evolution of the EM fields and electron-beam dynamics, assuming small signal modulation in the beam’s electron velocity and charge density. The beam electrons have average velocity and linear charge density u_0 and ρ_0 , respectively. The electron beam has an average (dc) current $I_0 = -\rho_0 u_0$ and

a dc (time-average) equivalent kinetic dc voltage $V_0 = \frac{1}{2}u_0^2/\eta$ [23,33], where $\eta = e/m = 1.758820 \times 10^{11}$ C/Kg is the charge-to-mass ratio of the electron with charge equal to $-e$ and rest mass m , and ρ_0 is negative. The small signal modulation in the electron-beam velocity and charge density u_b and ρ_b , respectively, form the so-called ‘‘charge wave.’’ The linearized basic equations governing charge motion and continuity are written in their simplest form as [16]

$$\begin{aligned} \partial_t u_b + u_0 \partial_z u_b &= -\eta e_z, \\ \partial_t \rho_b &= -\rho_0 \partial_z u_b - u_0 \partial_z \rho_b, \end{aligned} \quad (1)$$

where e_z is the electric field component in the z direction of the EM mode in the SWS interacting with the electron beam, and the operator ∂_σ indicates differentiation with respect to the variable σ . For convenience, we define the equivalent kinetic beam voltage and current as $v_b = u_b u_0 / \eta$ and $i_b = u_b \rho_0 + u_0 \rho_b$. Assuming an $e^{i\omega t}$ time dependence for monochromatic fields, the two equations in (1) are written in terms of the beam’s equivalent voltage and current in the phasor domain as

$$\begin{aligned} \partial_z V_b &= -i\beta_0 V_b - E_z, \\ \partial_z I_b &= -ig V_b - i\beta_0 I_b, \end{aligned} \quad (2)$$

where $\beta_0 = \omega/u_0$ is the beam equivalent propagation constant and $g = \frac{1}{2}I_0\beta_0/V_0$. Lowercase letters are used for the time-domain representation while capital letters are used for the phasor-domain representation. The details of the model used to describe the electron beam and its fundamental equations that describe the beam dynamics in space and time are given in Appendix A.

The EM mode propagating in the SWS is described by the equivalent transmission line in Fig. 1(b), with distributed per-unit-length series impedance Z and shunt admittance Y , and equivalent voltage $V(z)$ and current $I(z)$ phasors that satisfy the telegrapher’s equations

$$\begin{aligned} \partial_z V &= -ZI, \\ \partial_z I &= -YV + I_s. \end{aligned} \quad (3)$$

The term I_s in Eq. (3) accounts for the electron stream flowing in the SWS that loads the TL as a shunt displacement current according to [16,29,32] and whose expression is given by $I_s = -\partial_z I_b$. For the noninteractive EM system (i.e., when $I_s = 0$), the propagation constant and the characteristic impedance of the electromagnetic mode are given by $\beta_p = \sqrt{-ZY}$ and $Z_c = \sqrt{Z/Y}$, respectively. The two root solutions represent waves that propagate in opposite directions, i.e., both β_p and $-\beta_p$ are valid solutions because of reciprocity. In this paper we consider that the SWS supports either a ‘‘forward’’ or a ‘‘backward’’ mode. The modal propagation constant is a complex number,

$\beta_p = \beta_{pr} + i\beta_{pi}$, where $\beta_r\beta_i < 0$ for forward modes and $\beta_r\beta_i > 0$ for backward modes. For example, when the TL is supporting forward-wave propagation, both roots in β_p and Z_c must be taken as the principal square roots, so that their real part is positive. In this case β_p turns out to be in the fourth complex quadrant [34]. However, for the TL supporting backward-wave propagation, the root of $\beta_p = \sqrt{-ZY}$ is taken as the principle square root (resulting in a positive real part), while the root of $Z_c = \sqrt{Z/Y}$ is taken as the secondary square root (resulting in a negative real part). In this case β_p turns out to be in the first complex quadrant [34].

Based on Pierce’s model [16], the EM wave couples to the electron beam with its longitudinal electric field given by $E_z = -\partial_z V$. For convenience, we define a state vector $\Psi(z) = [V(z), I(z), V_b(z), I_b(z)]^T$ that describes the system evolution with coordinate z . Thus, the interacting EM mode and electron-beam’s charge wave are described as [32]

$$\partial_z \Psi(z) = -i\mathbf{M}\Psi(z), \quad (4)$$

where \mathbf{M} is the 4×4 system matrix

$$\mathbf{M} = \begin{bmatrix} 0 & -iZ & 0 & 0 \\ -iY & 0 & -g & -\beta_0 \\ 0 & -iZ & \beta_0 & 0 \\ 0 & 0 & g & \beta_0 \end{bmatrix}. \quad (5)$$

This description in terms of a multidimensional first-order differential equation in Eq. (4) is ideal for exploring the occurrence of EPDs in the system since an EPD is a degeneracy associated to two or more coalescing eigenmodes; hence, it occurs when the system matrix \mathbf{M} is similar to a matrix that contains a nontrivial Jordan block. In general, there are four independent eigenmodes, and each eigenmode is described by an eigenvector $\Psi(z)$; hence, it includes both the EM and the charge wave. At the EPD investigated in this paper two of these four eigenvectors coalesce.

III. SECOND-ORDER EPD IN AN INTERACTING ELECTROMAGNETIC WAVE AND AN ELECTRON-BEAM’S CHARGE WAVE

Assuming a state vector z -dependence of the form $\Psi(z) \propto e^{-ikz}$, where k is the wave number of a mode in the interacting system, i.e., in the hot SWS, the eigenmodes are obtained by solving the eigenvalue problem $k\Psi(z) = \mathbf{M}\Psi(z)$, and the modal dispersion relation is given by

$$\begin{aligned} D(\omega, k) &= \det(\mathbf{M} - k\mathbf{I}) \\ &= k^4 - 2\beta_0 k^3 + (\beta_0^2 + ZY - iZg)k^2 \\ &\quad - 2\beta_0 ZYk + \beta_0^2 ZY \\ &= 0. \end{aligned} \quad (6)$$

The solution of this equation leads to four modal complex wave numbers that describe the four modes in the EM electron-beam interactive system. A second-order EPD occurs when two of these eigenmodes coalesce in their eigenvalues and eigenvectors, which means that the matrix \mathbf{M} is similar to a matrix that contains a Jordan block of order two [20,21]. Following the theory in Ref. [35], the algebraic formulation that is often used to determine EPDs (and summarized in Appendix B) is equivalent to a bifurcation theory that is here applied. Indeed, the EPD radian frequency and wave number are simply obtained by setting $D(\omega_e, k_e) = 0$ and $\partial_k D(\omega_e, k)|_{k_e} = 0$ as in Ref. [35], where the EPD is designated with the subscript e . Based on the details provided in Appendix B these two conditions show that the EPD occurs when the transmission line per-unit-length series impedance and shunt admittance are $Z = Z_e$ and $Y = Y_e$, where

$$Z_e = \frac{i\beta_{0e}^2 \delta_e^3}{g_e}, \quad Y_e = \frac{ig_e(\delta_e + 1)^3}{\delta_e^3}, \quad (7)$$

and $\delta_e = (k_e - \beta_{0e})/\beta_{0e}$ represents the relative deviation of the degenerate modal wave number k_e (of the interactive system) from the beam's equivalent propagation constant $\beta_{0e} = \omega_e/u_0$.

Using the equations in (7), we constrain δ_e to provide Z_e and Y_e with positive real part, which means that we assume that the TL is passive because of SWS losses and especially because of the distributed-power-extraction mechanism (see Appendix B). In Fig. 2 we show the two sectoral regions of δ_e that allow EPDs for transmission line that support either forward or backward propagation. These two regions satisfy the passivity condition of the TL, $\text{Re}(Z) \geq 0$ and $\text{Re}(Y) \geq 0$, where the real parts of Z and Y represent mainly distributed power extraction (i.e., radiation losses using terminology from the antenna community). It is important to point out that the dark blue regions in Fig. 2 correspond to complex values of δ_e where the EPD is obtained for the TL that also has gain (independently of the electron beam). As explained in Appendix B, the two light blue and red narrow sectoral regions in Fig. 2 also correspond to an electron beam that delivers energy to the TL. In the rest of this paper we focus on the light blue region that represents complex values of δ_e associated to EPDs resulting from the interaction of a backward propagating electromagnetic wave and the charge wave modulating the electron beam. We stress that distributed radiated power is represented by series and/or parallel “losses” in the passive TL.

We now simplify the two equations given in (7) to get rid of δ_e as follows: from the first equation in (7) we find that $\delta_e = \sqrt[3]{-ig_e Z_e / \beta_{0e}^2}$, where the proper choice of root, based on the chart in Fig. 2, is the one that guarantees the passivity of the TL, and that there is power delivered from

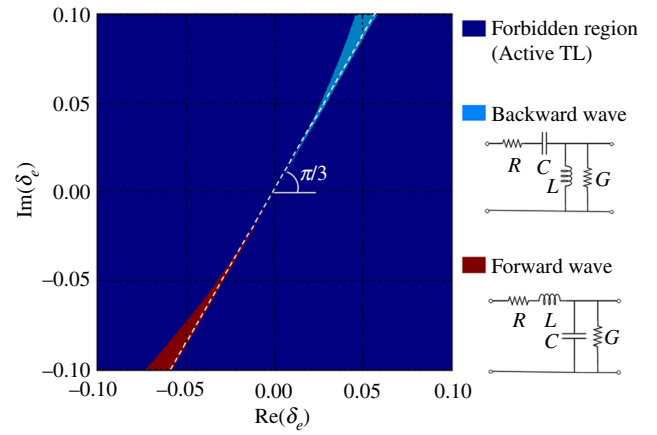


FIG. 2. The two sectoral regions represent complex values of δ_e , associated to EPDs resulting from the interaction of backward or forward electromagnetic waves (radiation is represented in the TL by series and/or parallel losses) and the charge wave of the electron beam. The value $\delta_e = (k_e - \beta_0)/\beta_0$ represents the wave number deviation of the EPD complex wave number k_e (of the interactive system) from the equivalent electron-beam wave number β_0 , which satisfies Eq. (7), assuming SWS realizations based on passive equivalent TLs. There are two regions of possible realizations (red and light blue), associated with the two distributed per-unit-length TL circuits shown in the right-hand panel, which represent SWSs supporting either forward- or backward-wave propagation. In this paper we focus on EPDs obtained from backward electromagnetic waves interacting with an electron beam, i.e., those leading to $\text{Re}(\delta_e) > 0$ and $\text{Im}(\delta_e) > 0$.

the beam to the TL (see Appendix B). For example, one of the roots of $\sqrt[3]{-ig_e Z_e / \beta_{0e}^2}$ should lie in the light blue region in the chart to have an EPD with passive TL that supports a backward wave. Roots of $\sqrt[3]{-ig_e Z_e / \beta_{0e}^2}$ that lie in the dark blue region are ignored because they would result in an EPD that requires an active TL, while here we consider only passive TLs because of power extraction. The EPD conditions in (7) are simplified by substituting the previous expression of δ_e in the second equation of (7), leading to an interesting equation that constrains the TL parameters and the electron-beam parameter g_e :

$$-Z_e Y_e / \beta_{0e}^2 = \left(\sqrt[3]{-ig_e Z_e / \beta_{0e}^2} + 1 \right)^3. \quad (8)$$

The above equation constrains all the system parameters to have an EPD; hence, it says that, for an EPD to occur, a specific choice of the electron-beam current $I_0 = I_{0e}$ and angular frequency $\omega = \omega_e$ must be selected. This is in good agreement with the general theory presented in Ref. [36] that indicates that a two-parameter family of complex matrices accounting for a strong coupling between eigenvalues possesses a double eigenvalue with the Jordan block, which defines the EPD. In other

words, it says that, for a given electron beam described by β_{0e} and g_e , the cold TL parameters Z_e and Y_e must be chosen accordingly. The condition in Eq. (8) can also be rewritten in term of the propagation constant β_{pe} and the characteristic impedance Z_{ce} of the cold TL as $(\beta_{pe}/\beta_{0e})^2 = \left(\sqrt[3]{g_e Z_{ce} \beta_{pe} / \beta_{0e}^2} + 1\right)^3$.

In general, the interaction between the charge wave and the EM wave occurs when they are synchronized, i.e., by matching the EM wave phase velocity ω/β_p to the average velocity of the electrons $u_0 = \omega/\beta_0$, a condition that is specifically called ‘‘synchronization.’’ Note that this is just an initial criterion, because the phase velocity of the modes in the *interactive* systems are different from ω/β_p and u_0 . When the system parameters are such that Eq. (8) is satisfied and hence an EPD occurs, there are two modes (in the interactive system) that have exactly the same phase velocity $\omega/\text{Re}(k_e)$. Since this synchronization condition corresponds to an EPD, the two modes in the interactive system are actually identical in their eigenvectors Ψ also. Note that the spatial z evolution of the interacting EM and electron charge wave is described by four modes that are solutions of Eq. (4), three of which have a positive real part of k , as discussed next and in Appendix B. At the EPD two of these four modes coalesce, i.e., they become identical, that is why we refer to this condition as ‘‘degenerate synchronization.’’ In this paper we explore and enforce this very special kind of synchronization based on an EPD. In particular, we enforce two of the resulting eigenmodes to fully coalesce in both their wave number and system state variable $\Psi(z)$. This condition is a different kind of EPD found in physical systems that does not satisfy PT symmetry since it involves the coupling between two different media of propagation, and may be very promising for achieving regimes of operation in electron-beam devices, with advantages not obtainable in conventional regimes.

The EPD condition obtained in Eq. (8) guarantees that the system has two repeated eigenvalues and two coalesced eigenvectors (see Appendix B),

$$\begin{aligned} k_e &= \sqrt[3]{\beta_{0e} \beta_{pe}^2}, \\ \Psi_e &= \left[1, \frac{ik_e}{Z}, \frac{1}{\delta_e}, \frac{g_e}{\beta_{0e} \delta_e^2} \right]^\top, \end{aligned} \quad (9)$$

which form the ‘‘degenerate synchronization.’’ For the interacting system of an EM wave and a charge wave, the EPD represents a point in parameter space at which the system matrix \mathbf{M} in Eq. (5) is not diagonalizable and it is indeed similar to a matrix that contains a 2×2 Jordan block. This implies that the solution of Eq. (4) includes an algebraic linear growth factor, resulting in unusual wave propagation characteristics, as discussed next.

The solution of Eq. (6) leads to four eigenmode wave numbers and, due to the highly nonreciprocal physical

nature of the electron beam, three have positive real part (i.e., $\text{Re}(k) > 0$) and one has negative real part. According to the traveling-wave tube theory in Refs. [16,28], conventionally applied to BWOs [22], these three distinct wave numbers with $\text{Re}(k) > 0$ participate to the synchronization mechanism, and the electric field in the SWS is generally represented as

$$V(z) = V_1 e^{-ik_1 z} + V_2 e^{-ik_2 z} + V_3 e^{-ik_3 z}. \quad (10)$$

Remarkably, at the EPD the interactive system has two modes with the same degenerate wave number k_e , resulting in a guided electric field with linear growth factor

$$V(z) = zV_1 e^{-ik_e z} + V_2 e^{-ik_e z} + V_3 e^{-ik_3 z}, \quad (11)$$

which is completely different from any other regime of operation. A degenerate mode described by Ψ_e is composed also of the charge wave, which implies that the charge wave propagation is also described as in (11), with two terms having the same degenerate wave number k_e , and one of them exhibiting the algebraic linear growth besides the exponential behavior.

In the following we show an example of degenerate synchronization based on an electron beam with dc voltage of $V_0 = 23$ kV and a dc current of $I_0 = 0.1$ A. We derive the system parameters assuming that the EPD electron-beam current $I_0 = I_{0e} = 0.1$ A (hence, the choice of the TL parameters are chosen accordingly) and that the operational frequency at which the EPD occurs is 1 GHz. We require (as an example) a relative degenerate wave number deviation of $\delta_e = 0.01 + i0.017$ that is lying exactly on the white dashed line shown in Fig. 2, with $\angle \delta_e = \pi/3$ (the phase of δ_e). The corresponding wave number of two coalescing modes in the interactive system is $k_e = (1 + \delta_e)\beta_{0e}$, which is $k_e = (1.01 + i0.017)\beta_{0e} = 70.55 + i1.21 \text{ m}^{-1}$. By imposing the beam parameters and the chosen δ_e in the EPD conditions in Eq. (7) we obtain the distributed per-unit-length TL impedance and admittance of the SWS to be $Z_e = -i257.1 \text{ Ohm m}^{-1}$ (i.e., capacitive) and $Y_e = 1 - i19.54 \text{ siemens m}^{-1}$ (i.e., inductive with losses), representing a backward wave in the SWS. Losses here are not modeling energy damping but rather energy extraction (e.g., radiation) from the TL, per unit length, like in a backward leaky wave antenna [37]. To obtain these values, we choose the per-unit-length TL parameters for backward-wave propagation as $C = 0.62 \text{ pFm}$, $L = 8.14 \text{ pHm}$, $R = 0 \text{ Ohm m}^{-1}$, and $G = 1 \text{ siemens m}^{-1}$. In Fig. 3(a) we show the dispersion relation of three complex modes in the ‘‘hot’’ SWS, i.e., in the interactive EM wave electron-beam system, obtained using the Pierce-based model as explained in Ref. [32]. [The fourth mode with $\text{Re}(k_e) < 0$ is not shown since it does not have a significant role in the synchronism.] We show the real and imaginary parts of the wave numbers of the three eigenmodes in the hot SWS versus the normalized frequency

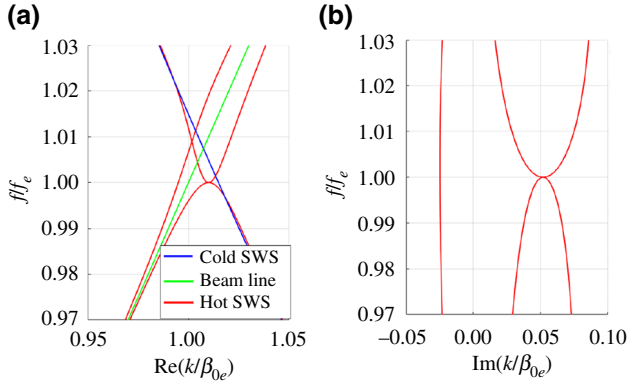


FIG. 3. Dispersion diagram for three of the four complex modes in the “hot” SWS (the modes in the SWS interacting with the electron beam), in red, showing the existence of a second-order EPD, where two modes coalesce in their wave numbers and eigenvectors. (a) Real part of the wave number of the modes phase propagating in the positive z direction [$\text{Re}(k_e) > 0$]. The blue line represents the dispersion of the EM mode in the cold SWS supporting a backward propagation, whereas the green line is the electron-beam’s charge wave dispersion, without accounting for their interaction. (b) Imaginary part of the wave number of the three modes with $\text{Re}(k_e) > 0$ resulting from the interaction. The EPD wave number at $f = f_e$ represents two fully degenerate and synchronous modes with exponential growth in z .

(red curves), together with the dispersion of the beam alone (i.e., the beam “line” in green that actually represents two curves since we are neglecting the effect of the beam plasma frequency here) and of the backward wave in the cold SWS (blue curve, with negative slope). It is obvious from the figure that two eigenmodes of the interactive system coalesce at the EPD frequency f_e , forming an EPD of order two. Each of these two eigenmodes has an EM wave and a charge wave counterpart, though far from the EPD frequency they tend to recover the beam line (green line) and the EM mode in the cold SWS (blue line).

We recall that the SWS is a periodic structure, and it is the slow wave harmonic of a mode that interacts with the electron-beam’s charge wave. Though slow waves do not radiate, a spatial Floquet-Bloch harmonic of the mode is fast and able to radiate through the slots [37], justifying the presence of the conductance $G = 1$ siemens m^{-1} , the real part of $Y_e = 1 - i19.54$ siemens m^{-1} , in the TL model.

IV. EPD-BWO THRESHOLD CURRENT

The EPD is here employed to conceive a regime of operation for BWOs based on “degenerate synchronization” between an EM wave and the electron beam. To explain this concept, we refer to the setup in Fig. 4(a) for a BWO that has “balanced gain and radiation loss” per unit length, where distributed loss is actually representing distributed radiation (per unit length) via a shunt conductance G (see Fig. 4). The description follows the steps outlined for

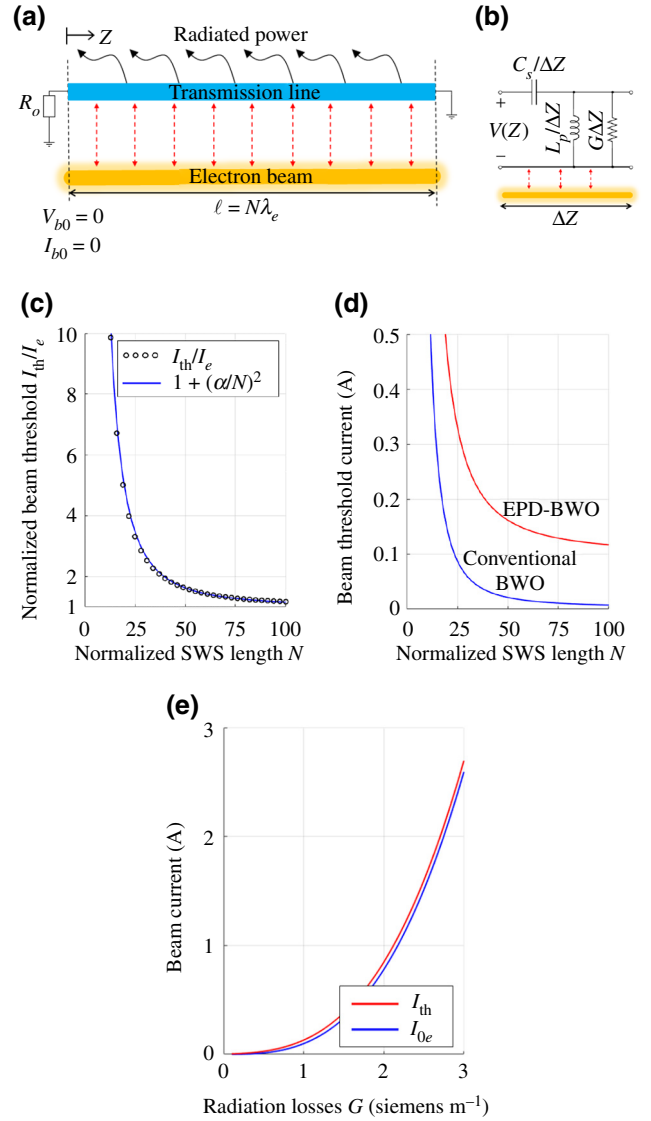


FIG. 4. (a) Schematic setup for BWOs with “balanced gain and radiation loss.” (b) Equivalent transmission line model of the SWS with distributed (per-unit-length) series capacitance and shunt inductance for a SWS that supports backward waves. The distributed shunt conductance G represents distributed power extraction, which is indeed given by $p_{\text{rad}}(z) = G|V(z)|^2/2$. (c) Scaling of the oscillation-threshold beam current I_{th} versus SWS length normalized to the wavelength $N = \ell/\lambda_e$, where $\lambda_e = 2\pi/\beta_{0e}$ is the guided wavelength calculated at the EPD frequency. It is obvious that, for infinitely long SWS where $N \rightarrow \infty$, we have $I_{\text{th}} \rightarrow I_{0e}$, which implies that the EPD synchronization condition is also the threshold for infinitely long SWSs. (d) Comparison of the threshold current for an EPD-BWO and a standard BWO for increasing SWS length. Note that the threshold of the EPD-BWO does not decrease to zero for longer SWSs, a characteristic that is fundamentally different from that of a standard BWO. (e) Scaling of the EPD beam current $I_0 = I_{0e}$ (blue curve) versus radiation losses G . We also show the scaling of the threshold beam current (red curve) for a finite-length SWS with $N = 70$. Note that the threshold beam current is very close to the EPD current for any amount of required distributed extracted power, which indicates that in principle the synchronism is achieved for any output power level.

BWOs in Refs. [16,22], where the TL is represented by the distributed circuit model shown in Fig. 4(b) that supports backward waves. An important difference from a standard BWO is that here the TL has shunt distributed “losses” that actually model the distributed radiation and whose presence is necessary to satisfy the EPD condition (8). We assume an unmodulated space charge at the beginning of the electron beam, i.e., $V_b(z=0) = 0$ and $I_b(z=0) = 0$, and we assume that the SWS waveguide length is $\ell = N\lambda_e$, where $\lambda_e = 2\pi/\beta_{0e}$ is the guided wavelength calculated at the EPD frequency and N is the normalized SWS length. We also assume that the SWS waveguide is terminated by a load at $z=0$ matched to the characteristic impedance of the TL (without loss and gain) $R_o = \sqrt{L/C}$ and by a short circuit at $z=\ell$. We follow the same procedure used in Ref. [22] to obtain the *starting oscillation condition* that is based on imposing infinite voltage gain $A_v = V(0)/V(\ell) \rightarrow \infty$. After simplification, and using the three-wave traveling-wave theory [16,22], the voltage gain is written in terms of the three modes concurring to the synchronization [those with $\text{Re}(k) > 0$] as

$$A_v^{-1} e^{i\beta_0 \ell} = \frac{e^{-i\beta_0 \delta_1 \ell} \delta_1^2}{(\delta_1 - \delta_2)(\delta_1 - \delta_3)} + \frac{e^{-i\beta_0 \delta_2 \ell} \delta_2^2}{(\delta_2 - \delta_3)(\delta_2 - \delta_1)} + \frac{e^{-i\beta_0 \delta_3 \ell} \delta_3^2}{(\delta_3 - \delta_1)(\delta_3 - \delta_2)} = 0, \quad (12)$$

where $\delta_n = (k_n - \beta_0)/\beta_0$ and k_1, k_2 , and k_3 are the three wave numbers of the interactive EM-beam system with positive real part that are solutions of Eq. (6). In close proximity of the EPD there are two modes coalescing, with $\delta_1 = \delta_a + \Delta/2$ and $\delta_2 = \delta_a - \Delta/2$, where $\delta_a = (\delta_1 + \delta_2)/2$ is the average, and $|\Delta| \ll |\delta_a|$ is a very small quantity that vanishes at the EPD. By observing that $|e^{-i\beta_0 \delta_3 \ell}| \ll 1$ for very large ℓ because $\text{Im}(k_3) < 0$, the gain expression in Eq. (12) reduces to

$$A_{ve}^{-1} e^{i\beta_0 \ell} \approx \frac{e^{-i\beta_0 \delta_a \ell} \delta_a^2 \sin(\Delta\beta_0 \ell/2)}{(\delta_a - \delta_3) \Delta/2} = 0. \quad (13)$$

From the above condition, assuming very large ℓ , the first oscillation frequency occurs when $\Delta\beta_0 \ell = 2\pi$. This happens when the constraint on the wave numbers $k_1 - k_2 = 2\pi/\ell$ is satisfied. This shows a very important fact that, for an infinitely long structure $\ell \rightarrow \infty$, the starting oscillation condition is $k_1 = k_2 = k_e$, which corresponds to the EPD condition. This implies that the EPD is the exact condition for synchronization between the charge wave and EM wave, accounting for the interaction in infinitely long SWSs that guarantees the generation of oscillations at the EPD frequency $f_e = \omega_e/(2\pi)$.

For finite length SWS, oscillations occurs when $k_1 - k_2 = 2\pi/\ell$ is satisfied, assuming very large ℓ , and since

$|\Delta| \ll |\delta_a|$, we have both k_1 and k_2 very close to k_e , which implies that the systems is close to the EPD and hence the threshold beam current I_{th} that starts oscillations is slightly different from I_{0e} . A beam current slightly away from the EPD one causes the wave numbers to bifurcate from the degenerate one k_e , following the Puiseux series approximation [38] (also called the fractional power expansion) as

$$k_n - k_e \approx (-1)^n \alpha \sqrt{I_0 - I_{0e}} \quad (14)$$

with $n = 1, 2$ and α a constant. This implies that $k_1 - k_2 \approx -2\alpha \sqrt{I_0 - I_{0e}}$, and by comparing this with the $k_1 - k_2$ difference associated to the threshold beam current in a finite length SWS, we infer that the threshold beam current I_{th} that makes the EPD-BWO of finite length ℓ oscillate, asymptotically scales as

$$I_{th} \sim I_{0e} + \left(\frac{\pi/\alpha}{\ell} \right)^2. \quad (15)$$

In a conventional BWO that has no distributed power extraction and the power is delivered only to the load R_0 , the threshold current scales asymptotically with the SWS length as $I_{th} \sim \zeta/\ell^3$ [22,39], where ζ is a constant. Instead, the EPD-BWO has a threshold current in Eq. (15) always larger than the EPD beam current I_{0e} , which represents the current that keeps the oscillation going and simultaneously balances the distributed radiated power. Importantly, the EPD beam current I_{0e} can be engineered to any desired (high) value depending on how much power one wants to extract from the electron beam.

The above derivation is based on assuming that $\ell \rightarrow \infty$ (see the details given in Appendix D), and a rigorous derivation for any length of the EPD-BWO SWS is shown in Appendix C that leads to the determination of the threshold current and oscillation frequency. This Pierce-based formulation for the beam current threshold is used to compute the results shown in Fig. 4 for varying the EPD-BWO length and the shunt conductance G that represents the distributed radiation.

In Fig. 4(c) we show the scaling of the threshold current versus SWS length for a system with the same parameters used in the previous example. The scaling shows that, for infinitely long SWSs, the oscillation starting current is equal to the EPD beam current I_{0e} , which is consistent with the asymptotic relation in Eq. (15). In Fig. 4(d) we also show a comparison between the threshold current of the conventional BWO (which does not have distributed power extraction, i.e., $G = 0$) and that of the EPD-BWO (with distributed power extraction, represented by $G = 1$ siemens m^{-1}) by showing their current scaling with the SWS length. The threshold beam current I_{th} of the conventional BWO vanishes when the SWS length increases, whereas the threshold beam current I_{th} of the EPD-BWO

tends to the value $I_{0e} = 0.1$ A. In Fig. 4(e) we show the threshold beam current $I_0 = I_{0e}$ (blue curve) that leads to the EPDs as a function of the radiation “loss” per unit length G . We also show the required starting beam current (i.e., the threshold) for oscillations (red curve) for a finite length “hot” SWS working at the EPD; we assume that the SWS length normalized to the wavelength at the EPD frequency is $N = 70$. It is important to point out that the radiated power per unit length of the SWS is determined using $p_{\text{rad}}(z) = \frac{1}{2}G|V(z)|^2$; thus, it is linearly proportional to the parameter G , i.e., higher values of G imply higher radiated power per unit length and therefore a higher level of energy extraction from the SWS.

We have shown two very important facts here. First, the threshold beam current is very close to the EPD beam current for any desired value of power extracted. This indicates that the EPD condition for hot SWSs with finite length is the condition that basically guarantees full synchronization between the EM guided mode and the beam’s charge wave. Second, the threshold current increases monotonically when increasing the required radiated power per unit length, which implies a tight synchronization regime guaranteed for any high power generation. Therefore, in principle, according to a Pierce-based model, the synchronism is maintained for any desired power output, and this trend is not observed in conventional BWOs where the load is at the beginning or end of the SWS.

V. CONCLUSION

We conceptually demonstrate the occurrence of an EPD in an interactive system made of a linear electron beam and a guided electromagnetic wave. This EPD condition leads to a regime of operation for BWOs where the EPD guarantees a synchronism between a backward wave and a beam’s charge wave through enforcing the coalescence of two modes in both their wave number and state vector, a regime we name “degenerate synchronization.” A remarkable aspect of this EPD-BWO regime is that the “gain and distributed-power-extraction balance” condition leads to a perfect degenerate synchronization between the charge wave and EM wave for any amount of designed distributed power extraction. This distributed power extraction can be in the form of distributed radiation from the interaction zone or of distributed transfer of power from the hot SWS to an adjacent coupled waveguide. Under this EPD-BWO regime, in principle, it is possible to extract large amounts of power from the electron beam and therefore the EPD-BWO exhibits a high starting beam current. In theory the starting-oscillation beam current (i.e., the threshold) could be set to arbitrary large values, in contrast to what happens in conventional BWOs where the beam’s starting current tends to vanish when the SWS length increases. Remarkably, in the EPD-BWO regime the starting oscillation current is always larger than the EPD’s beam current

that, in principle, can be set to large values by increasing the amount of power extracted per unit length. Therefore, we have shown the fundamental principle that the amount of power generated under the EPD-BWO regime has no upper limit (the actual limit would be imposed only by the constraints encountered in the practical realizability), contrarily to conventional knowledge of BWOs.

Note that the degenerate synchronization regime discussed in this paper is very different from those discussed in Refs. [24–27]. There, it was the “cold” SWS that exhibited a degeneracy condition, like the degenerate band edge, which is an EPD of order four, or the stationary inflection point (SIP), which is an EPD of order three, that were proposed to enhance the performance of high power devices. Those DBE and SIP EPD conditions were obtained in “cold” SWSs based on periodicity, and indeed the interaction of the EM modes with the electron beam would perturb those degeneracy conditions, and even destroy them for increasingly large values of electron-beam currents. Here, instead, we propose a fully synchronous degenerate regime based on the concept of “distributed radiation and gain balance,” where the EPD occurs in the “hot” structure, i.e., in the presence of the interacting electron beam with any amount of current and hence, in principle, for any large amount of power.

ACKNOWLEDGMENT

This material is based upon work supported by the Air Force Office of Scientific Research under Grant No. FA9550-18-1-0355.

APPENDIX A: ELECTRON-BEAM MODEL

We show the fundamental equations that describe the evolution of electron-beam dynamics in space and time. We follow the linearized equations that describe the space-charge wave on the electron beam presented in Pierce [16] based on the electron-beam model in Ref. [15]. We assume a narrow cylindrical beam of electrons subject to axial electric field that is constant across the beam’s cross section; we assume purely longitudinal electron motion, as conventionally done in many electron-beam devices thanks to confinement due to an applied magnetic field, and negligible repulsion forces between electrons (hence we neglect space charge’s induced forces) compared to the force induced by the longitudinal electric field associated to the radio-frequency mode in the slow wave structure (this last assumption could be easily removed). The beam’s total linear-charge density and electron speed are represented as

$$\rho(z, t) = \rho_0 + \rho_b, \quad u(z, t) = u_0 + u_b, \quad (\text{A1})$$

where the subscripts “0” and “b” denote dc (average value) and ac (alternate current, i.e., modulation), respectively, ρ_0

here is negative, and u is the electron speed in the z direction. The basic equations governing the charges' motion and continuity are written in their simplest form as [16]

$$\frac{du}{dt} = -\eta e_z, \quad (\text{A2a})$$

$$\frac{\partial \rho}{\partial t} = -\frac{\partial(\rho u)}{\partial z}, \quad (\text{A2b})$$

where $\eta = e/m = 1.758\,820 \times 10^{11}$ C/Kg is the charge-to-mass ratio of the electron, the electron charge is equal to $-e$ and m is its rest mass. Assuming small signal modulation [15,29], $|u_b| \ll u_0$ and $|\rho_b| \ll |\rho_0|$, Eqs. (A2) are linearized to

$$\frac{\partial u_b}{\partial t} + u_0 \frac{\partial u_b}{\partial z} = -\eta e_z, \quad (\text{A3a})$$

$$\frac{\partial \rho_b}{\partial t} = -\rho_0 \frac{\partial u_b}{\partial z} - u_0 \frac{\partial \rho_b}{\partial z}. \quad (\text{A3b})$$

For convenience, we define the equivalent kinetic beam voltage and current [16] as

$$v(z, t) = \frac{u^2}{2\eta} = V_0 + v_b, \quad (\text{A4a})$$

$$i(z, t) = u\rho = -I_0 + i_b. \quad (\text{A4b})$$

Again, assuming small signal modulation [15,29], $|u_b| \ll u_0$ and $|\rho_b| \ll \rho_0$, we neglect the terms u_b^2 and $u_b\rho_b$ in Eqs. (A4). Thus, the dc and ac beam voltages and currents are determined as a function of the dc and ac beam charge densities and speeds [16,23,33] as

$$V_0 = \frac{1}{2}u_0^2/\eta, \quad (\text{A5a})$$

$$I_0 = -\rho_0 u_0, \quad (\text{A5b})$$

$$v_b = u_b u_0 / \eta, \quad (\text{A5c})$$

$$i_b = u_b \rho_0 + u_0 \rho_b. \quad (\text{A5d})$$

By substituting Eqs. (A5) into Eqs. (A3), the evolution equations of beam equivalent kinetic voltage and current are written as

$$\frac{\partial v_b}{\partial z} = -\frac{1}{u_0} \frac{\partial v_b}{\partial t} - e_z, \quad (\text{A6a})$$

$$\frac{\partial i_b}{\partial z} = \frac{\eta \rho_0}{u_0^2} \frac{\partial v_b}{\partial t} - \frac{1}{u_0} \frac{\partial i_b}{\partial t}. \quad (\text{A6b})$$

Assuming time-harmonic signals with time convention $e^{i\omega t}$, which is omitted in the following for simplicity,

Eqs. (A6) are simplified to their phasor version:

$$\frac{\partial V_b}{\partial z} = \frac{-i\omega}{u_0} V_b - E_z, \quad (\text{A7a})$$

$$\frac{\partial I_b}{\partial z} = \frac{i\omega \eta \rho_0}{u_0^2} V_b - \frac{i\omega}{u_0} I_b. \quad (\text{A7b})$$

When the electron beam is not interacting with an electromagnetic wave, i.e., when $E_z = 0$, the charge wave has propagation constant $\beta_0 = \omega/u_0$.

APPENDIX B: SECOND-ORDER EPD IN A SYSTEM MADE OF AN ELECTROMAGNETIC WAVE INTERACTING WITH AN ELECTRON-BEAM'S CHARGE WAVE

The solution of the dispersion equation in Eq. (6) has four roots that represent the eigenvalues of the interactive system composed of guided EM waves and the charge waves that modulate the electron beam. A necessary condition to have second-order EPD is to have two repeated eigenvalues, which means that the characteristic equation should have two repeated roots as

$$D(\omega_e, k) \propto (k - k_e)^2, \quad (\text{B1})$$

where ω_e and k_e are the degenerate angular frequency and wave number, respectively. The relation in Eq. (B1), which guarantees having two coalescing wave numbers, is satisfied when [35]

$$D(\omega_e, k_e) = 0, \quad (\text{B2a})$$

$$\left. \frac{\partial D(\omega_e, k)}{\partial k} \right|_{k=k_e} = 0. \quad (\text{B2b})$$

Substituting the determinant expression (6) into Eqs. (B2), the two EPD conditions are

$$k_e^4 - 2\beta_{0e} k_e^3 + (\beta_{0e}^2 + Z_e Y_e - i g_e Z_e) k_e^2 - 2\beta_{0e} Z_e Y_e k_e + \beta_{0e}^2 Z_e Y_e = 0, \quad (\text{B3})$$

$$4k_e^3 - 6\beta_{0e} k_e^2 + 2(\beta_{0e}^2 + Z_e Y_e - i g_e Z_e) k_e - 2\beta_{0e} Z_e Y_e = 0, \quad (\text{B4})$$

where the EPD is designated with the subscript e , i.e., the parameters with the subscript e are calculated at the EPD frequency; for example, $\beta_{0e} = \omega_e/u_0$. Only at a specific frequency (the EPD frequency) is it possible to find two identical eigenvalues. Therefore, the above equations provide both the EPD radian frequency ω_e and wave number k_e .

The combination of the TL distributed series impedance $Z = Z_e$ and shunt admittance $Y = Y_e$ that provide the EPD

are determined after making some mathematical manipulations in the two conditions in Eqs. (B3) and (B4). First, we use Eq. (B3) to get Y_e in terms of Z_e and other system parameters as

$$Y_e = \frac{ig_e k_e^2}{(k_e - \beta_{0e})^2} - \frac{k_e^2}{Z_e}, \quad (\text{B5})$$

then we substitute this relation into Eq. (B4) and solve for Z_e , which is found to be

$$Z_e = \frac{i(k_e - \beta_{0e})^3}{\beta_{0e} g_e}. \quad (\text{B6})$$

We finally substitute Z_e into Eq. (B5) to obtain

$$Y_e = \frac{ig_e k_e^3}{(k_e - \beta_{0e})^3}. \quad (\text{B7})$$

These two latter expressions are then rewritten as in (7). Assuming that the EPD conditions in Eqs. (B6) and (B7) are satisfied, the degenerate wave number k_e is determined by the product of Eqs. (B6) and (B7), $Z_e Y_e = -k_e^3/\beta_{0e}$, and by recalling that $Z_e Y_e = -\beta_{pe}^2$, leading to $k_e = \sqrt[3]{\beta_{0e} \beta_{pe}^2}$, which is the result in (9).

The eigenvectors Ψ_n of the system are determined by solving

$$(\underline{\mathbf{M}} - k_n \mathbf{I}) \Psi_n = \mathbf{0}, \quad (\text{B8})$$

where k_n with $n = 1, 2, 3, 4$ are the modal wave numbers, and they are determined from Eq. (6). By solving Eq. (B8), the eigenvectors are written in the form (each element of the eigenvector carries an implicit unit of volt besides the units of the explicit parameters)

$$\Psi_n = \left[1, \frac{ik_n}{Z}, \frac{1 + \delta_n}{\delta_n}, \frac{g(1 + \delta_n)}{\beta_{0e} \delta_n^2} \right]^T, \quad (\text{B9})$$

where $\delta_n = (k_n - \beta_0)/\beta_0$. As shown in Ref. [16], three of these four modes are strongly affected by the synchronization of the electron beam and the EM mode with positive phase velocity. Assuming that these three wave numbers of the beam-EM mode interactive system are a slight perturbation of the unperturbed beam's propagation constant, i.e., $k_n \approx \beta_0$ with $n = 1, 2, 3$, the eigenvector expression in Eq. (B9) is approximated as

$$\Psi_n \approx \left[1, \frac{ik_n}{Z}, \frac{1}{\delta_n}, \frac{g}{\beta_{0e} \delta_n^2} \right]^T. \quad (\text{B10})$$

It is worth mentioning that the eigenvector expression in Eq. (B9) is valid for any of the four modes of the interacting system, whereas the expression in Eq. (B10) is only

valid for the three modes with positive $\text{Re}(k)$, namely, for the three synchronous modes resulting from the interaction of the SWS EM mode with the electron beam. Those three synchronous modes are such that $k_n \approx \beta_0$ based on synchronization. Two of these eigenvectors coalesce at the EPD, forming the degenerate synchronism between the two modes $\Psi_1 = \Psi_2 = \Psi_e$, where

$$\Psi_e \approx \left[1, \frac{ik_e}{Z}, \frac{1}{\delta_e}, \frac{g_e}{\beta_{0e} \delta_e^2} \right]^T. \quad (\text{B11})$$

In summary, the two conditions in (7) represent constraints on the TL parameters, calculated at the EPD frequency, which provide the second-order EPD, where two eigenmodes of the interacting system have identical eigenvalues $k_1 = k_2 = k_e$ and eigenvectors $\Psi_1 = \Psi_2 = \Psi_e$. These two eigenmodes form the degenerate synchronization.

From the transmission line point of view, the electron beam is modeled as parallel per-unit-length admittance

$$Y_b = \frac{-igk^2}{(k - \beta_0)^2} \quad (\text{B12})$$

that loads the line [32]. For proper operation of this degenerate BWO regime, the TL should outcouple power in a distributed fashion and the electron beam should supply power to balance the power extraction in order to have a sustainable oscillation. This means that both the TL parameters Z and Y should be passive, i.e., $\text{Re}(Z) > 0$ and $\text{Re}(Y) > 0$, and the beam equivalent admittance should be active, i.e., $\text{Re}(Y_b) < 0$. These constraints are plotted in Fig. 5 as a function of the complex wave number deviation $\delta_e = (k_e - \beta_{0e})/\beta_{0e}$. The intersection of these three conditions on $\text{Re}(Z) > 0$ and $\text{Re}(Y) > 0$, and $\text{Re}(Y_b) < 0$ lead to the realizability diagram in Fig. 5(d), which is the same as in Fig. 2.

APPENDIX C: BACKWARD-WAVE OSCILLATOR THRESHOLD CURRENT

For a finite SWS with length ℓ , the equivalent voltage that describes the electric field at any coordinate z in the SWS is expanded as a combination of the four modes supported by the interactive beam-EM mode system (modes are calculated in a SWS of infinite length) as

$$V(z) = V_1 e^{-ik_1 z} + V_2 e^{-ik_2 z} + V_3 e^{-ik_3 z} + V_4 e^{-ik_4 z} \quad (\text{C1})$$

where k_n with $n = 1, 2, 3, 4$ are the modes' wave number determined from Eq. (6), and the V_n are the complex mode amplitudes. The associated TL current and beam dynamics are found by using Eq. (C1) in Eq. (4) or by using the

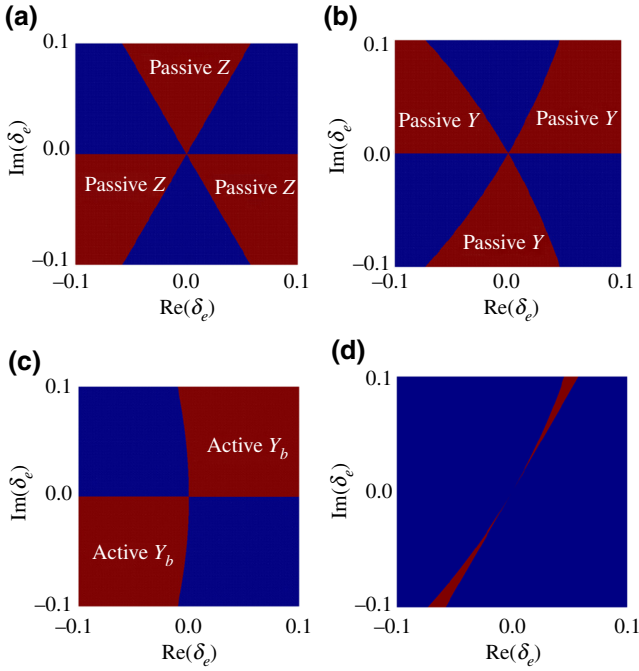


FIG. 5. Regions of complex values δ_e that result in having passive TL, with $\text{Re}(Z) > 0$ and $\text{Re}(Y) > 0$ when EPD conditions are satisfied, i.e., when $Z = Z_e$ and $Y = Y_e$: (a) passive series impedance $\text{Re}(Z_e) = \text{Re}(i\beta_{0e}^2 \delta_e^3 / g_e) > 0$ and (b) passive parallel admittance $\text{Re}(Y_e) = \text{Re}(ig_e(\delta_e + 1)^3 / \delta_e^3) > 0$. (c) Regions of complex values δ_e where the electron beam delivers energy to the TL, i.e., when the electron beam provides gain from the TL perspective, which means that $\text{Re}(Y_{be}) < 0$, i.e., $\text{Re}(-ig(1 + \delta_e)^2 / \delta_e^2) < 0$. (d) Regions satisfying the (a), (b), and (c) realizability criteria.

eigenvector expression in Eq. (B9):

$$I(z) = \frac{ik_1 V_1}{Z} e^{-ik_1 z} + \frac{ik_2 V_2}{Z} e^{-ik_2 z} + \frac{ik_3 V_3}{Z} e^{-ik_3 z} + \frac{ik_4 V_4}{Z} e^{-ik_4 z}, \quad (\text{C2a})$$

$$V_b(z) = \frac{(1 + \delta_1) V_1}{\delta_1} e^{-ik_1 z} + \frac{(1 + \delta_2) V_2}{\delta_2} e^{-ik_2 z} + \frac{(1 + \delta_3) V_3}{\delta_3} e^{-ik_3 z} + \frac{(1 + \delta_4) V_4}{\delta_4} e^{-ik_4 z}, \quad (\text{C2b})$$

$$I_b(z) = \frac{g(1 + \delta_1) V_1}{\beta_0 \delta_1^2} e^{-ik_1 z} + \frac{g(1 + \delta_2) V_2}{\beta_0 \delta_2^2} e^{-ik_2 z} + \frac{g(1 + \delta_3) V_3}{\beta_0 \delta_3^2} e^{-ik_3 z} + \frac{g(1 + \delta_4) V_4}{\beta_0 \delta_4^2} e^{-ik_4 z}. \quad (\text{C2c})$$

Here $\delta_n = (k_n - \beta_0) / \beta_0$. The setup we use for the BWO with distributed power radiation, shown in Fig. 4(a), is similar to that used in Ref. [22], where we assume unmodulated space charge at the beginning of the electron beam [i.e., $V_b(z=0) = 0$ and $I_b(z=0) = 0$], and we

also assume that the output power is extracted at $z = 0$, terminated with a resistance matched to the characteristic impedance of the TL (without loss and gain) $R_o = \sqrt{L/C}$, and short circuit at $z = \ell$, where $\ell = N\lambda_e$ is the SWS length (i.e., the TL length) and $\lambda_e = 2\pi / \beta_{0e}$ is the guided wavelength calculated at the EPD frequency. [Note that in the absence of loss and gain in the TL, the TL distributed series impedance and shunt admittance are $Z = 1/(i\omega C)$ and $Y = 1/(i\omega L)$.] The boundary conditions that describe the mentioned setup are

$$V(0) + R_o I(0) = 0, \quad (\text{C3a})$$

$$V(\ell) = 0, \quad (\text{C3b})$$

$$V_b(0) = 0, \quad (\text{C3c})$$

$$I_b(0) = 0. \quad (\text{C3d})$$

By imposing Eqs. (C2) in Eqs. (C3), we obtain a homogeneous system of linear equations that is written in matrix form as

$$\mathbf{A}(\omega, I_0) \mathbf{V} = \mathbf{0}, \quad (\text{C4})$$

where $\mathbf{V} = [V_1, V_2, V_3, V_4]^T$. Free oscillation in the interactive system occurs when there is a solution of Eq. (C4) despite the absence of the source term [the right-hand side of Eq. (C4) is equal to zero]. Therefore, oscillation occurs for a combination of radian frequency and electron-beam current that satisfies

$$\det[\mathbf{A}(\omega, I_0)] = 0. \quad (\text{C5})$$

Since the solution of the above equation defines the threshold beam current to start oscillations, such a solution is denoted by $I_0 = I_{\text{th}}$, and $\omega = \omega_{\text{res}}$ is the frequency of the oscillation.

APPENDIX D: ASYMPTOTIC SCALING OF THE EPD-BWO THRESHOLD BEAM CURRENT

In this section we derive the oscillation condition and the asymptotic scaling of the threshold beam current with the SWS length for the proposed EPD-BWO assuming that the length of the structure tends to infinity. We follow the traveling-wave tube theory used in Refs. [16,22,28], since the synchronization involves mainly three waves, those with $\text{Re}(k_n) > 0$. Assuming that these three wave numbers have a slight variation of the unperturbed beam wave number, i.e., $k_n \approx \beta_0$, we use the eigenvector expression in Eq. (B10) to write the TL circuit voltage and beam dynamics distribution along the z direction, which are represented

in terms of three modes as [22]

$$V(z) = V_1 e^{-ik_1 z} + V_2 e^{-ik_2 z} + V_3 e^{-ik_3 z}, \quad (\text{D1a})$$

$$V_b(z) = \frac{V_1}{\delta_1} e^{-ik_1 z} + \frac{V_2}{\delta_2} e^{-ik_2 z} + \frac{V_3}{\delta_3} e^{-ik_3 z}, \quad (\text{D1b})$$

$$I_b(z) = \frac{gV_1}{\beta_0 \delta_1^2} e^{-ik_1 z} + \frac{gV_2}{\beta_0 \delta_2^2} e^{-ik_2 z} + \frac{gV_3}{\beta_0 \delta_3^2} e^{-ik_3 z}, \quad (\text{D1c})$$

where $\delta_n = (k_n - \beta_0)/\beta_0$. The wave numbers k_n , $n = 1, 2, 3$, have positive real part with two (say $n = 1, 2$) having positive imaginary part and the third ($n = 3$) having negative imaginary part. A numerical example of the wave numbers is shown in Fig. 3. Here, we follow the same procedure used in Ref. [22] to obtain the oscillation condition that is based on imposing infinite voltage gain $A_v = V(0)/V(\ell) \rightarrow \infty$. By imposing the beam boundary condition $V_b(0) = 0$ and $I_b(0) = 0$ in Eqs. (D1) and after some mathematical manipulations, the gain expression is written in its simplest form as [22]

$$\begin{aligned} A_v^{-1} e^{i\beta_0 \ell} &= \frac{e^{-i\beta_0 \delta_1 \ell} \delta_1^2}{(\delta_1 - \delta_2)(\delta_1 - \delta_3)} + \frac{e^{-i\beta_0 \delta_2 \ell} \delta_2^2}{(\delta_2 - \delta_3)(\delta_2 - \delta_1)} \\ &\quad + \frac{e^{-i\beta_0 \delta_3 \ell} \delta_3^2}{(\delta_3 - \delta_1)(\delta_3 - \delta_2)} \\ &= 0. \end{aligned} \quad (\text{D2})$$

We first neglect the term with $e^{-i\beta_0 \delta_3 \ell}$ in Eq. (D2) since we consider a very large SWS length ℓ and know that $\text{Im}(\delta_3) < 0$. Therefore, the gain expression reduces to

$$A_v^{-1} e^{i\beta_0 \ell} \approx \frac{e^{-i\beta_0 \delta_1 \ell} \delta_1^2}{(\delta_1 - \delta_2)(\delta_1 - \delta_3)} + \frac{e^{-i\beta_0 \delta_2 \ell} \delta_2^2}{(\delta_2 - \delta_3)(\delta_2 - \delta_1)}. \quad (\text{D3})$$

By defining $\Delta = (\delta_1 - \delta_2)$, and hence $\delta_1 = \delta_a + \Delta/2$ and $\delta_2 = \delta_a - \Delta/2$, where $\delta_a = (\delta_1 + \delta_2)/2$ is the average, the gain expression is then written as

$$A_v^{-1} e^{i\beta_0 \ell} \approx e^{-i\beta_0 \delta_a \ell} \left(\frac{(\delta_a + \Delta/2)^2 e^{-i\beta_0 \Delta \ell/2}}{(\Delta/2)(\delta_a - \delta_3 + \Delta/2)} + \frac{(\delta_a - \Delta/2)^2 e^{i\beta_0 \Delta \ell/2}}{(\Delta/2)(\delta_a - \delta_3 - \Delta/2)} \right), \quad (\text{D4})$$

In close proximity of the EPD we know that two modes coalesce, i.e., $\delta_1 \approx \delta_2$; thus, we can assume that $|\Delta| \ll |\delta_a|$, i.e., $\Delta \rightarrow 0$ as we approach the EPD. It is important to point out that, although Δ is a very small value, we cannot neglect its effect in the exponential function in Eq. (D4) because we assume the SWS to be very long; however, we can neglect Δ in other places, i.e., we have $\delta_a \pm \Delta/2 \approx \delta_a$ and $\delta_a - \delta_3 \pm \Delta/2 \approx \delta_a - \delta_3$. Thus, the gain expression finally reduces to Eq. (13). The first oscillation frequency

occurs when the constraint on the wave numbers $k_1 - k_2 = 2\pi/\ell$ is satisfied. A beam current slightly away from the EPD one causes the wave numbers to bifurcate from the degenerate one k_e , following the Puiseux series approximation [38] as $k_1 - k_2 \approx -2\alpha\sqrt{I_0 - I_{0e}}$, where α is a constant. Therefore, the threshold beam current is determined by solving $2\alpha\sqrt{I_{\text{th}} - I_{0e}} = -2\pi/\ell$, which yields the asymptotic trend for the scaling of threshold current in Eq. (15).

This asymptotic trend is confirmed in Fig. 4, where the threshold current I_{th} is calculated numerically by solving $\det[\mathbf{A}(\omega, I_0)] = 0$ for the beam current I_0 , as discussed in Appendix C.

-
- [1] M. V. Berry, Physics of nonhermitian degeneracies, *Czech. J. Phys.* **54**, 1039 (2004).
 - [2] C. M. Bender and S. Boettcher, Real Spectra in non-Hermitian Hamiltonians Having PT Symmetry, *Phys. Rev. Lett.* **80**, 5243 (1998).
 - [3] W. Heiss, M. Müller, and I. Rotter, Collectivity, phase transitions, and exceptional points in open quantum systems, *Phys. Rev. E* **58**, 2894 (1998).
 - [4] R. El-Ganainy, K. Makris, D. Christodoulides, and Z. H. Musslimani, Theory of coupled optical PT-symmetric structures, *Opt. Lett.* **32**, 2632 (2007).
 - [5] A. Guo, G. Salamo, D. Duchesne, R. Morandotti, M. Volatier-Ravat, V. Aimez, G. Siviloglou, and D. Christodoulides, Observation of PT Symmetry Breaking in Complex Optical Potentials, *Phys. Rev. Lett.* **103**, 093902 (2009).
 - [6] S. Bittner, B. Dietz, U. Günther, H. Harney, M. Miski-Oglu, A. Richter, and F. Schäfer, PT-Symmetry and Spontaneous Symmetry Breaking in a Microwave Billiard, *Phys. Rev. Lett.* **108**, 024101 (2012).
 - [7] H. Kazemi, M. Y. Nada, T. Mealy, A. F. Abdelshafy, and F. Capolino, Exceptional Points of Degeneracy Induced by Linear Time-Periodic Variation, *Phys. Rev. Appl.* **11**, 014007 (2019).
 - [8] T. Mealy, A. F. Abdelshafy, and F. Capolino, in *2019 United States National Committee of URSI National Radio Science Meeting (USNC-URSI NRS M)* (IEEE, Boulder, CO, USA, 2019), p. 1.
 - [9] A. Figotin and I. Vitebskiy, Oblique frozen modes in periodic layered media, *Phys. Rev. E* **68**, 036609 (2003).
 - [10] A. Figotin and I. Vitebskiy, Gigantic transmission band-edge resonance in periodic stacks of anisotropic layers, *Phys. Rev. E* **72**, 036619 (2005).
 - [11] A. Figotin and I. Vitebskiy, Frozen light in photonic crystals with degenerate band edge, *Phys. Rev. E* **74**, 066613 (2006).
 - [12] M. A. Othman, X. Pan, G. Atmatzakis, C. G. Christodoulou, and F. Capolino, Experimental demonstration of degenerate band edge in metallic periodically loaded circular waveguide, *IEEE Trans. Microw. Theory Tech.* **65**, 4037 (2017).

- [13] M. Y. Nada, M. A. Othman, and F. Capolino, Theory of coupled resonator optical waveguides exhibiting high-order exceptional points of degeneracy, *Phys. Rev. B* **96**, 184304 (2017).
- [14] J. T. Sloan, M. A. Othman, and F. Capolino, Theory of double ladder lumped circuits with degenerate band edge, *IEEE Trans. Circuits Syst. I: Regular Papers* **65**, 3 (2018).
- [15] D. Bohm and E. P. Gross, Theory of plasma oscillations. A. Origin of medium-like behavior, *Phys. Rev.* **75**, 1851 (1949).
- [16] J. Pierce, Waves in electron streams and circuits, *Bell Syst. Tech. J.* **30**, 626 (1951).
- [17] R. C. Hansen, *Phased Array Antennas* (John Wiley & Sons, NJ, USA, 2009). Vol. 213.
- [18] W. L. Stutzman and G. A. Thiele, *Antenna Theory and Design* (John Wiley & Sons, NY, USA, 2012).
- [19] Wei Wang, Shun-Shi Zhong, Yu-Mei Zhang, and Xian-Ling Liang, A broadband slotted ridge waveguide antenna array, *IEEE Trans. Antennas Propag.* **54**, 2416 (2006).
- [20] M. A. Othman and F. Capolino, Theory of exceptional points of degeneracy in uniform coupled waveguides and balance of gain and loss, *IEEE Trans. Antennas Propag.* **65**, 5289 (2017).
- [21] A. F. Abdelshafy, M. A. Othman, D. Oshmarin, A. T. Almutawa, and F. Capolino, Exceptional points of degeneracy in periodic coupled waveguides and the interplay of gain and radiation loss: Theoretical and experimental demonstration, *IEEE Trans. Antennas Propag.* **67**, 6909 (2019).
- [22] H. R. Johnson, Backward-wave oscillators, *Proc. IRE* **43**, 684 (1955).
- [23] S. E. Tsimring, *Electron Beams and Microwave Vacuum Electronics* (John Wiley & Sons, NJ, USA, 2007).
- [24] M. A. Othman, M. Veysi, A. Figotin, and F. Capolino, Low starting electron beam current in degenerate band edge oscillators, *IEEE Trans. Plasma Sci.* **44**, 918 (2016).
- [25] M. A. Othman, M. Veysi, A. Figotin, and F. Capolino, Giant amplification in degenerate band edge slow-wave structures interacting with an electron beam, *Phys. Plasmas* **23**, 033112 (2016).
- [26] A. F. Abdelshafy, M. A. Othman, F. Yazdi, M. Veysi, A. Figotin, and F. Capolino, Electron-beam-driven devices with synchronous multiple degenerate eigenmodes, *IEEE Trans. Plasma Sci.* **46**, 3126 (2018).
- [27] M. A. Othman, V. A. Tamma, and F. Capolino, Theory and new amplification regime in periodic multimodal slow wave structures with degeneracy interacting with an electron beam, *IEEE Trans. Plasma Sci.* **44**, 594 (2016).
- [28] J. Pierce, Theory of the beam-type traveling-wave tube, *Proc. IRE* **35**, 111 (1947).
- [29] S. Ramo, Space charge and field waves in an electron beam, *Phys. Rev.* **56**, 276 (1939).
- [30] R. Kompfner, The traveling-wave tube as amplifier at microwaves, *Proc. IRE* **35**, 124 (1947).
- [31] L. J. Chu and J. D. Jackson, Field theory of traveling-wave tubes, *Proc. IRE* **36**, 853 (1948).
- [32] V. A. Tamma and F. Capolino, Extension of the pierce model to multiple transmission lines interacting with an electron beam, *IEEE Trans. Plasma Sci.* **42**, 899 (2014).
- [33] A. Gilmour, *Klystrons, Traveling Wave Tubes, Magnetrons, Crossed-Field Amplifiers, and Gyrotrons* (Artech House, MA, USA, 2011).
- [34] R. W. Ziolkowski and E. Heyman, Wave propagation in media having negative permittivity and permeability, *Phys. Rev. E* **64**, 056625 (2001).
- [35] G. W. Hanson, A. B. Yakovlev, M. A. Othman, and F. Capolino, Exceptional points of degeneracy and branch points for coupled transmission lines—Linear-algebra and bifurcation theory perspectives, *IEEE Trans. Antennas Propag.* **67**, 1025 (2019).
- [36] A. Seyranian, O. Kirillov, and A. Mailybaev, Coupling of eigenvalues of complex matrices at diabolic and exceptional points, *J. Phys. A: Math. Gen.* **38**, 1723 (2005).
- [37] D. R. Jackson and A. A. Oliner, in *Modern Antenna Handbook* (John Wiley & Sons, New York, 2008), p. 325.
- [38] A. Welters, On explicit recursive formulas in the spectral perturbation analysis of a Jordan block, *SIAM J. Matrix Anal. Appl.* **32**, 1 (2011).
- [39] L. Walker, Starting currents in the backward-wave oscillator, *J. Appl. Phys.* **24**, 854 (1953).